Object Searching, Acquisition, and Classification Using Stabilized Thermal Imaging on Smart UAVs for Use in Low-Cost SAR Applications

Technical Report #CSSE2202-01

O'Leary, Houston
Bemidji State University
houston.oleary@live.bemidjistate.edu

Vasquez, Mariana
University of California, Berkeley
marianavasquez@berkeley.edu

Velumani, Swarna
University of Maryland, College Park
sveluman@terpmail.umd.edu

Biaz, Saad
Auburn University
biazsaa@auburn.edu

Chapman, Richard
Auburn University
chapmro@auburn.edu

August 1, 2024

Abstract

Modern developments in Unmanned Aerial Vehicles (**UAVs**) and Artificial Intelligence provides new opportunities for research in search and rescue (**SAR**) domains. Integrating thermal imaging with these developments allows search and rescue teams to find their target(s) in environments where using visible spectrum imaging becomes a challenge (e.g. foliage cover, smoke or gas, during the hours of night). To build on this problem, we implement object searching and detection techniques in conjunction with stabilized thermal imagery to build an operational search system for finding missing persons in a low-cost SAR scenario. Our object detection model consists of a Single-Shot Detector (**SSD**) pre-trained on the 2017 COCO image dataset and retrained on a publicly available thermal imaging data set equipped for the task of localizing an object in the image and performing classification. In addition to object detection, we propose a search model that integrates traditional SAR tactics like the Euclidean distance rings with lost person behavior and map generation within a Deep Q-Learning Network (**DQN**) model to search for a missing person(s) inside an established local coordinate reference frame. The proposed project uses a hexa-copter UAV equipped with a developed 2-axis gimbal stabilizer and a comparatively low-cost thermal imaging camera to test the object classification and search algorithm.

1 Introduction

Every year, it is approximated that 4,080 individuals become lost in the United States. In Yosemite National Park alone, 393 search incidents were reported from 2000 to 2010. In response to lost persons, a search and rescue (**SAR**) operation is conducted which costs nearly 51.4 million dollars annually [4]. SAR operations are not only expensive, but can also be physically and mentally taxing for the rescuers. Furthermore, these rescuers must maximize their limited time to save a lost person because after the first 24 hours, the probability of survival drops to 75 percent. This means that finding these missing persons early is crucial to search and rescue teams and communities. However, due to the often challenging terrain in the environments where these individuals are most commonly lost, it can sometimes be difficult to locate the missing person(s) within that short 24 hour period of time. This challenge presents the opportunity for the use of unmanned aerial vehicles (**UAVs**) within the search and rescue domain. By implementing the use of UAVs, search and rescue teams can avoid the difficulties of searching over rough terrain and, when coupled with the use of thermal imaging, can spot lost persons through obscurities to visible light cameras such as fog, foliage, or smoke.

Utilizing UAVs equipped with long-wave infrared (**LWIR**) thermal imaging capabilities in search and rescue scenarios has become an increasingly sought after approach by search and rescue teams. However, many of today's unmanned aerial vehicle platforms equipped with LWIR thermal imaging capabilities can cost search and rescue teams and/or consumers a considerable amount of money leaving their applications limited to those who have the required amount of resources to do so. This makes studying the viability of comparatively low-cost systems critical so that search and rescue teams who lack the exorbitant amount of resources can still utilize unmanned aerial vehicles in SAR scenarios.

Introducing artificial intelligence and autonomy into this application of UAVs can benefit search and rescue teams by allowing for a systematic and easily repeatable approach to emerge. Furthermore, employing smart unmanned aerial vehicles (**SUAVs**) in SAR operations can reduce the amount of necessary supervision and also allows the SUAVs to take advantage of additional information that can be used to search for missing persons more effectively. Recent advances in deep learning software have given rise to the implementation of reinforcement learning search algorithms such as Deep Q-Learning [6] on SUAVs in which the UAV itself learns the best path for search from the environment and a reward system. Performing object detection techniques such as localization and subsequent classification on thermal imagery data captured by the UAV can be used to alert the search and rescue teams when the lost individual has been found.

This paper aims to provide a start to finish solution for the application of smart unmanned aerial vehicles (**SUAVs**) equipped with stabilized thermal imaging capabilities within a low-cost search and rescue scenario. This includes the optimized search of the target, and detection/classification of the target. The rest of the paper will be organized as follows. In section 2 [2] we will discuss past related work. Section 3 [3] will describe the UAV platform and hardware, next we will discuss path planning in section 4 [4]. Section 5 [5] will discuss the simulation used in this research to test our path planning algorithm, and the remaining sections will indicate the results [6], conclusion, and future work [7] in that order.

2 Related Works

2.1 Lost Person Behavior Modeling

Advances in search theory and informative path planning have led to numerous approaches for effectively narrowing the shortest search path to the target. One such work includes a simulated lost person behavior model that is used in conjunction with a human searcher behavior model built off a collection of data from past SAR missions [3]. All together, the models are used to produce a probabilistic heat map of the target's location and possible search paths. A Gaussian process assesses risk to optimally elect the final UAV path.

Koester's book on Lost Person Behavior introduced the SAR's community to the idea of categorizing lost people into certain behavior profiles based on various factors such as occupation, age, and experience. Trying to model lost person behavior is a growing field of interest and a recent paper [7] has attempted to build a probability mass function (**PMF**) based on the six known lost person reorientation strategies. Since lost-person behavior profiles correlate with the terrain such as elevation and linear features, a map is generated using United States Geological Survey (**USGS**) data. The geophysical characteristics included are water bodies, railroads, trails, and elevation. All possible permutations of the behavior strategies are generated as PMF's and the probability of each is increased by one. From this set only the PMF's that sum to one are kept and simulated for 500 Monte Carlo replicates for each incident from International Search and Rescue Incident Database (**ISRID**). The best behavior profile for each incident is the one with the lowest energy statistic. To formulate the final PMF, each incident's profile is given a weight and then combined to find the average behavioral profile.

For a hiker, the resulting behavioral profile was [RW, RT, DT, SP, VE, BT] =[0.055,0.377,0.559,0.003,0.006,0]. The result was validated using leave-one-out cross validation that showed 58.5% of the total initial planning points (**IPP**) have energy statistic values above the 95th percentile, and 98.5% above the 50th percentile. The tested IPP's are not just those of hikers but of any lost person which goes to show the PMF works well on more than half of the SAR incidents it was not trained on.

Another work [1] that tackles lost person behavior modeling uses a Decision Tree Algorithm (DTA) coupled with a heuristic path finding algorithm to anticipate a lost person's movement in the wilderness-context. The DTA takes in multiple inputs including energy state, mental state, objects in view, and strategy state to output a strategy/destination. This project is limited to 3 strategies due to the terrain map only working with elevation, but in reality Koester has outlined 6 total decision strategies. Two heuristic path finding algorithms are tested: the Kitchens Equation, which takes into consideration elevation changes and distance to the goal, and the Bellman Equation which estimates the probability of a hiker moving to a tile based on expended energy in kilo calories. The Bellman equation simulation reached its target much faster than the Kitchens equation. Also, the Kitchen's equation focused on saddle points of the terrain and moving between these points which is not always the most accurate in real world SAR scenarios.

2.2 Deep Q-Learning Network

In [12], a multi-agent reinforcement learning algorithm is proposed for the purposes of search and rescue with multiple UAVs. The paper includes the addition of Long Short Term Memory (LSTM) neural network layers to function despite imperfect information or partial observability. For the evaluation, the framework was compared to other common algorithms such as Multi-Agent Q-Learning and Multi-Agent Deep Q-Learning in AirSim simulator. Our work extends to this through the use of continuous action space or image-based environments where we utilize AirSim in conjunction with Ardupilot SITL. Additionally, we use thermal imaging rather than visible light images due to their utility in SAR scenarios and real world testing.

Another work uses an approximate form of reinforcement learning known as Partially Observable Markov Decision Processes and uses AirSim simulator along with Keras, the machine learning framework [15]. The reinforcement learning network used is DQN with the addition of Hindsight Experience Replay which increases the efficiency of learning such that intermediate states are associated with reward and the agent can learn even from episodes that fail. While for the DQN, a sparse reward function was chosen with the aim of simply finding the object, our proposal aims to incorporate expert knowledge on lost person behavior and information on the surrounding terrain to find the optimal search path for each particular SAR operation. Another drawback was the lack of variation in the AirSim environments used for training whereas our project also receives real world training and testing in addition to simulation.

2.3 Object Detection

Target acquisition is a critical task in SAR operations where the lost person should be located as quickly as possible to receive aid. Other works have used a variety of methods to localize and classify objects from image input data in scenarios similar to SAR. In one such work, [2] equipped their drone with an onboard object detection pipeline to complete a set of tasks from the Mohamed Bin Zayed International Robotics Challenge 2020 (e.g. capturing a ball, spotting and popping balloons, locating and moving a brick). The pipeline uses an encoder-decoder structure for contour detection of generic foreground objects from Pascal VOC dataset. Standard ResNet, with less layers to reduce the level of computation, was used for its CNN architecture that detects object contours at multiple scales together with their orientations.

Another work focusing on an image processing techniques to classify a person's state of consciousness used Faster R-CNN (region-based convolutional neural networks), a common object detection model that identifies regions of interest where objects are expected to be found and then does detection within those

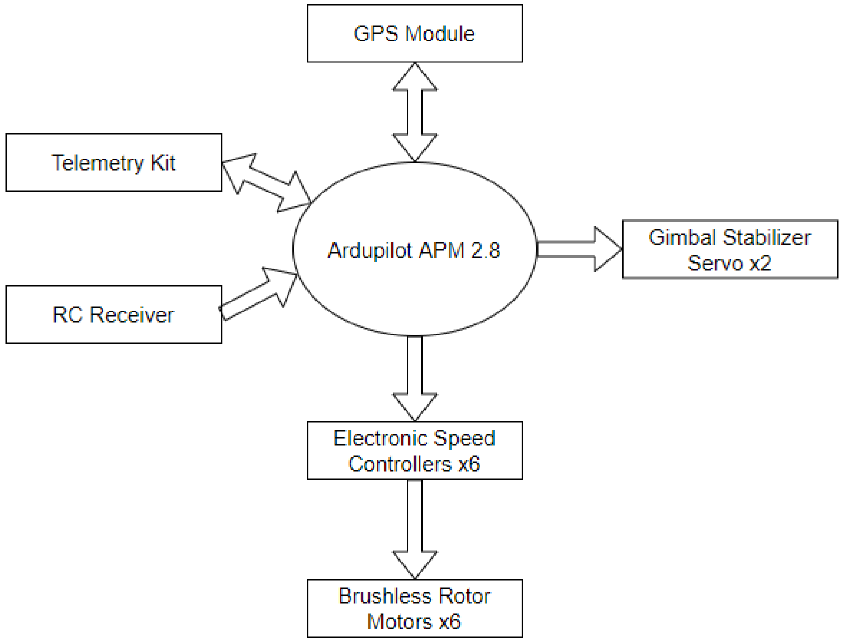

Figure 1: Block Diagram of sUAV Platform

regions [11]. Yet another work concerned with putting together a high-altitude thermal image dataset for UAVs tested their images with the object detection model YOLOv4 (You Only Look Once) [14]. Region proposal algorithms such as R-CNN perform slower with slightly better accuracy while single-shot algorithms such as YOLO and SSD are much faster and more practical for real-time detection with a minimal drop in accuracy.

One paper made a direct comparison between some of the popular object detection models and found that SSD strikes the best balance between speed and accuracy as it is faster than R-CNN and achieves better accuracy when compared to YOLO [10]. Experimental results demonstrated that the SSD model is better in human detection application when compared with the previously used methods such as HOG method and the Haar Cascade method and had a faster processing speed in terms of frames per second.

3 Platform and Hardware

The UAV platform used in this research is largely a DIY hobbyist drone platform that can be recreated through comparatively simple means. Figure [1] represents the block diagram of the system while figure [2] depicts the UAV itself. This hexa-copter is assembled mainly for autonomous flight, but is also capable of being controlled manually through remote control (RC) input channels as well. The main pieces of hardware used to assemble this platform are as follows: one Ardupilot Mega 2.8 APM Flight Controller, one eight channel RC receiver, a 2.4GHz telemetry kit, a 5.8GHz audio/video transmitter, a GPS module, six brush-less electronic propeller motors, and six electronic speed controllers to control those motors.

The Ardupilot Mega 2.8 APM flight controller is the main controlling component of this platform and is what makes most of the autonomous flight possible. The APM FCU is a complete open source autopilot system that can be acquired at a relatively low cost and is largely based on the ATMEGA328P micro-

Figure 2: UAV Platform

controller. Users can create way-point missions for the drone either through scripts or through a Ground Control Station (GCS) software. Within the flight controller is a 3-axis gyroscope sensor, accelerometer, magnetometer, and barometer. As the name suggests, this flight control unit (FCU) is compatible with Arduino and has full MavLink support as well.

Figure three [3] depicts our developed 2-axis gimbal stabilizer that will be mounted to the bottom of the UAV. One of the bigger challenges within this field of research is attaining stable and clear imaging from a UAV mid-flight and using a low-cost, low-resolution thermal imaging camera such as the one used in this project only exacerbates the problem. The developed 2-axis gimbal was designed to minimize this problem as much as possible so that we could attain stable and clear imaging for use in information processing. ArduPilot has direct support for gimbal stabilization of up to three axes and if servo motors are used, the connecting of the servos is very simple and intuitive. The gimbal piece parts themselves were designed inside a 3D modeling software and were fabricated using a hobbyist Fused Deposition Modeling (FDM) printer. The material or filament used in the fabrication of the gimbal was a thermoplastic called Polyethylene Terephthalate Glycol, commonly known as PET-G within the FDM printing community. This material was chosen mainly due to its cost effectiveness, but also its significant chemical resistance and durability as well. The thermal imaging camera we purchased that will be mounted onto the gimbal is a FLIR Vue Pro. The camera variant employed in this project comes with a resolution of 336x256 and a refresh rate of 7.5Hz.

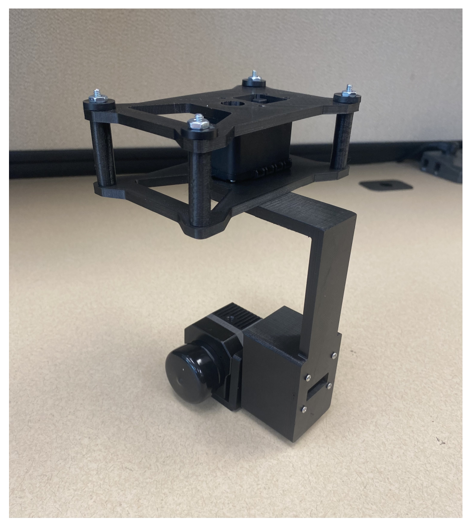

Figure 3: Video Retrieval

In order to retrieve aerial video data from the camera, we purchased a 5.8GHz Audio/Video transmitter and developed a wiring circuit that would allow us to connect the transmitter to the FLIR Vue Pro thermal imaging camera. The wiring circuit will subsequently be described in detail and is also depicted in Figure 4 [4]: First, the video data retrieval system will be powered by a separate power supply from the rest of the platform in order to maximize the flight time of the SUAV. This was done using two 7.4 volt, 1350mAh LiPo (Lithium-Polymer) Batteries connected in parallel. The power supply is connected to the 600mW, 40-channel Audio/Video transmitter which is able to supply power to the camera as well as receive analog

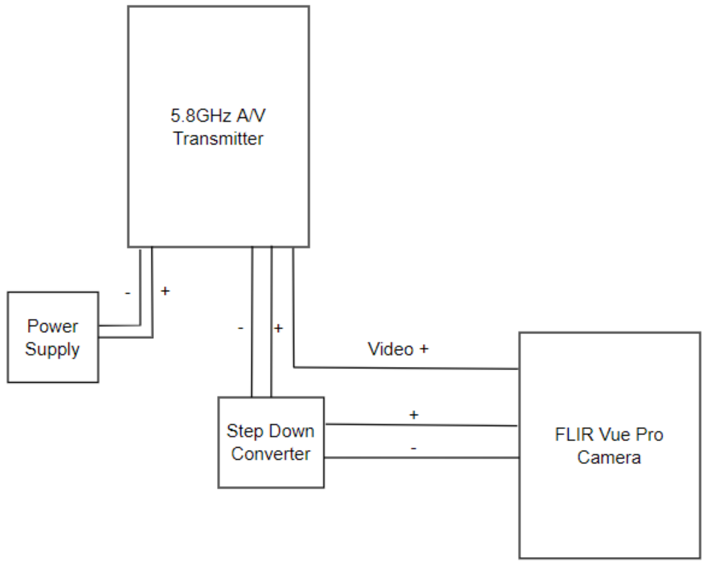

Figure 4: Transmitter Wiring Diagram

video data from the camera. In our case, a DC to DC step down converter was also needed due to the fact that the FLIR Vue Pro input power is rated for 5 volts and the transmitter outputs the same level of voltage it receives from the power supply to the camera (7.4 volts in our case). The transmitter takes the information it receives from the camera and converts that into radio signals which is then sent out into the air via the antenna. The GCS (ground control station) coordinator then captures the radio signals using an Audio/Video receiver which converts the signals back into video data which can then subsequently be used for information processing. It is recommended that a receiver equipped with channel scanning capabilities be used in order to achieve the highest image quality as possible.

4 Path Planning

4.1 Lost Person Behavior

One of the most crucial steps of a SAR's operation is creating an effective search plan that capitalizes on methods to better understand lost person behavior. A lost person is defined as someone who cannot determine their current location and does not have the facilities to reorient themselves to a known direction[8]. Dudchenko describes two ways a person may end up being lost: misorientation and disorientation [5]. Misorientation is when a person is in a familiar location but is exposed to different elements within said location. For instance, bad weather may obscure a known landmark, and the absence of a reorientation strategy can lead to someone being lost. Another form of misorientation is when a person believes they are headed in the right direction and does not take into account slight changes in the environment. Essentially, misorientation is when an individual maintains spatial awareness of certain landmarks, but their direction is completely incorrect. Disorientation is when someone does not have this spatial awareness therefore creating a disconnect between direction and distance. The lost person really has no idea on how to self-localize because their perception of where landmarks exist is inaccurate.

In *Lost Person Behavior*, Koester has outlined multiple lost person categories also known as Subject Categories or Lost Person Types (**LPT**) that are based on different demographics such as age, cognitive or emotional state, occupation, and activities performed prior to being lost. These categories have proven to share similar reorientation strategies, motivation, and energy statistics which can be extremely useful to SAR teams when predicting a specific lost person. For instance, a hiker is more likely to follow predetermined paths and take into account roads and trails, whereas a dementia patient or even a child may travel in a straight line. These categories are created from real-world SAR statistics part of the International Search and Rescue Incident Database (**UAVs**). In SAR missions, LPT's are incorporated in probability distribution maps to increase the likelihood of finding a lost person in a shorter time frame. One of the oldest, yet most effective path planning strategies used today is the Euclidean Distance Rings. These rings map 25%, 50%, 75%, and 95% quantiles for the Euclidean distance between the Initial Planning Point (**IPP**) and the find location[13]. Koester designates different distance cutoffs based on the Subject Category and terrain. In our research we focus on hikers because it is the most researched and has more data points to test and train. Not only does Koester introduce revolutionary ideas like Subject Categories and integrating them into Euclidean Distance Rings, but also different reorientation strategies. In our research we work with six of them:

1.Random Walking (RW): An agent does not follow has no set guiding rule and has equal probability of moving in any direction.

2.Route Traveling (RT): An agent follows some predetermined path like a trail.

3.Direction Traveling (DT): An agent moves in one body-direction which means ignoring any signs or trials.

4.Staying Put (SP): An agent stays in the same location.

5.View Enhancing (VE): An agent attempts to gain height to increase their POV

6.Backtracking (BT): An agent traces their step back towards an earlier location.

Lost persons can practice any of these strategies and are not restricted to only one while navigating to a known location. Hikers tend to practice DT more than any other reorientation strategy with RT and RW coming in second and third. However, among hikers 32-48% will be found uphill in relation to the IPP [9]. This shows that VE is still a likely strategy lost hikers may use to gain a vantage point advantage. In fact, a recent phenomenon in lost persons is to move uphill, even if it goes against the rule of least resistance, to gain a cell signal [9]. These patterns of a lost person subgroup can be extremely beneficial in path planning.

4.2 Effects of Topography and Linear Features

Location can greatly impact decisions taken by a lost person. For instance, elevation is one of the greatest navigating factors a lost person may use. Studies show that a third of lost hikers travel uphill in hopes of improving their field of view, but most lost people follow the path of least resistance even if it means traveling the Manhattan Distance to avoid any steep hills or sloping terrain. In addition, hikers tend to stick to linear features such as trails when lost. This preference for easier and clear paths, coupled with a limited knowledge of their surroundings, limits the number of destinations the person may consider. Being able to extract linear features and topographical information would lead to a more informed search therefore maximizing the limited time in real-world SAR scenarios.

4.3 Map Generation

In this section, we describe how the 2D map was created to be used as the state space in the DQN model. These maps were created with two main goals 1) to find linear features a hiker may follow 2) determine inaccessible or hard to reach areas. The first layer is elevation/topography data taken from UCSD with an accuracy of 11.1 meters. Next, the way points are calculated based on the GSD of the camera, and the coordinate grid is split into cells with each cell being 2 km * 2 km. The way points are set to be the center of each cell and hold the elevation level of the nearest coordinate point from the UCSD data set. The next three layers included are National Hiking Trails and rivers. The National Hiking Trails and Rivers are ArcGis shape files that were converted from LineStrings to Coordinate Points. Each way point iterates through the Trails and Roads coordinate arrays to determine if the respective cell holds any of these features.

4.4 Deep Q-Learning Network

In a reinforcement learning problem, a training agent interacts with the environment. For our purposes, the training agent will be the drone and the environment for simulation is our chosen environment in AirSim (and the real world during real world testing). Each subsequent action taken by the agent leads to a state and each state-action pair is associated with its own positive or negative reward. The goal for the agent is to maximize reward across an episode or the duration of the game from the starting state to the terminal state. During training, the agents goes through many episodes to learn the best policy which refers to the best set of actions to take in order to maximize reward. Our reinforcement learning problem must follow the Markov property which makes the assumption that each state depends only on the state that directly precedes it. Keeping the dependencies to a minimum allows for feasible computation, especially in games with large state spaces.

$$Q(s, a) = R(s, a) + \gamma \max_{a} Q(s', a)$$

Across an episode we aim to accumulate the highest amount of reward so we wish to maximize our total reward in the form of a Q-value. In a SAR scenario, our reward is determined by a lost person behavior model and the generated maps of the search space. The defined reward function should encourage the drone to mimic the behavior of a lost person and choose the route of least resistance given the information it holds of the surrounding environment. The above equation demonstrates how each Q-value is determined by the reward at the current state and the discounted future Q-value where the subsequent Q-value is calculated by maximizing over the possible action to take from the current state. Modifying the discount factor or value of gamma will decide the contribution of future rewards in relation to the current reward. The update rule for determining the optimal Q-value is as follows:

$$Q(s, a) \leftarrow Q(s, a) + \alpha[R(s', a) + \gamma \max_{a} Q(s', a) - Q(s, a)]$$

The learning rate or value of alpha determines the balance of exploration versus exploitation. Ideally, the learning rate should be initialized to a value such that the agent focuses on exploration during the training process and change in value such that the policy learned during exploration can be exploited. Given the computational intensity of our problem and the large state space, we opted to use deep q-learning. Rather than updating a table of state-action pairs and their respective Q-values, deep q-learning uses a neural network where the states act as input for the problem.

4.5 Reward System

The novelty of our research stems from incorporating lost person behavior modeling within a DQN framework. We enhance the DQN model for lost hikers in the wilderness environment by modifying the reward algorithm to take into account the 6 reorientation strategies discussed in [9]. Each strategy is given a weight(w) based off of the PMF function from the average profile of a hiker in [7]. In decision theory, a branch of study that makes decisions by assigning probabilities to a list of factors and weighing gain and loss based on the outcome, includes an optimal decision-making approach to multi-criteria decision analysis (MCDA) problems known as the weighted sum model (WSM). WSM is when there are multiple alternatives and we have to choose the best option based on a certain criteria. The best option is found by calculating the

WSM score. This score is found by assigning weights to every factor and then taking the linear combination of every factor's weight multiplied by the actual value. If there are n criteria and R is the reward for a cell (i) in the coordinate grid, then the reward would be the WSM score which is calculated as follows:

$$R_i^{WSM_{score}} = \sum_{j=1}^{n} w_j a_{ij}$$

By including all 6 of the reorientation strategies as constraints we allow for the possibility of a lost hiker to choose a different one at every time step. Now, our weights are the numbers found for an average hiker profile based on ISRID which is [RW, RT, DT, SP, VE, BT] =[0.055,0.377,0.559,0.003,0.006,0].The performance value (a) is either 1 or -1 based on the corresponding weight/reorientation strategy it is multiplied with. In our training we follow these associations:

Random Walking (RW):

- 0.055(+1) - constant or decreasing altitude

- 0.055(-1) - increasing altitude

Route Traveling (RT):

- 0.377(+1) - cell contains a linear feature

- 0.377(-1) - cell does not contain a linear feature

Directional Traveling (DT):

- 0.559(+1) - traveling in the same direction

- 0.559(-1) - changing trajectory

Staying Put (SP):

- 0.003(+1) - stay in the same cell

- 0.003(-1) - leave the cell

View Enhancing (VE):

- 0.006(+1) - altitude increase

- 0.006(-1) - altitude decrease

4.6 Object Detection

A Single-Shot Detector (SSD) object detection model pretrained on 2017 COCO image dataset and retrained on the OSU Thermal Pedestrian Dataset is used to perform localization and classification of the lost person with the thermal imaging input data. The OSU Thermal Pedestrian Dataset is divided into ten sequences where each sequence is a series of thermal images taken on the Ohio State University campus. The model uses a training to testing split of 80:20 such that 227 images are for training and 57 for testing from the 284 image dataset. The camera used to capture the images of the dataset had a Raytheon 300D thermal sensor core with a 75mm lens and was mounted on an eight story building at the time of data collection. The 360 by 240 pixel images are of pedestrian intersections across the Ohio State University campus. Although not completely uniform, the sampling rate for the sequences was about 30 Hz. Ground truth was included in the form of bounding box coordinates and class of which the dataset contains only one: person. People who were less than 50 percent visible were excluded from the annotations. The 2017 COCO dataset contains over 200k labeled visible light images with 80 object categories. Object detection combines computer vision

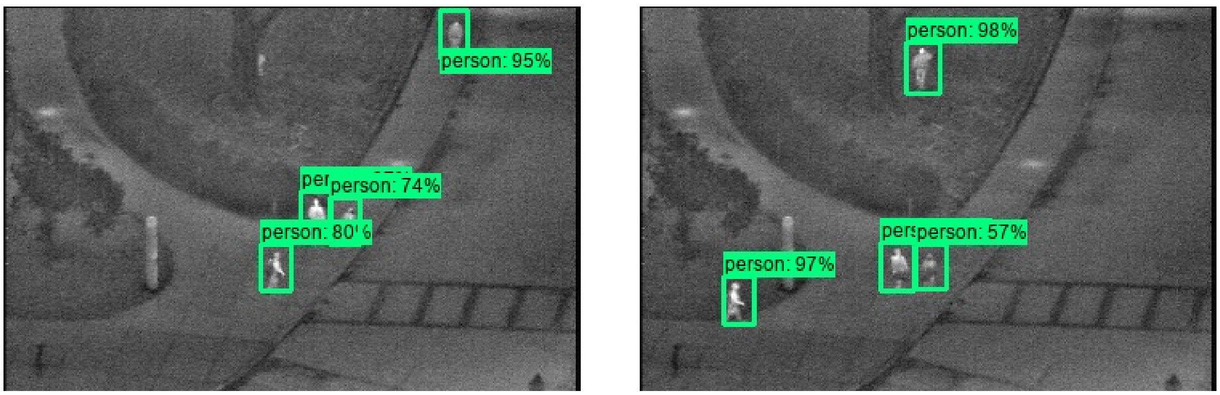

(a) Sample 1 Train

(b) Sample 2 Train

Figure 5: Object Detection Retraining

tasks: object localization and image classification. In relation to the search algorithm, being able to detect a lost person from the thermal image input data we will receive from the drone will allow us to know when we have reached the goal state or when we have completed our search. The pretrained SSD model used was taken from the TensorFlow Model Garden. The structure of the model includes a backbone and a SSD head where the backbone is generally a pretrained image classification network excluding the final output layer and the SSD head adds more convolutional layers to form the output of bounding boxes and classes for the objects detected in the image. In our case, the backbone is extracted from MobileNet, an image classification model designed to be used for mobile applications for its lightweight architecture.

5 Simulation

One of the goals in this research in testing the path planning algorithm was to use a simulation that would be directly transferable to a real world application. Meaning that any scripts written for testing the path planning within the simulation could also be implemented on a real world UAV. In order to do so, we decided to use ArduPilot SITL (software in the loop) in conjunction with Microsoft AirSim. The integration of the two pieces software was just recently developed in 2019 and was originally developed to run natively on Linux. ArduPilot SITL is a piece of open-source software that allows you to simulate a real

world UAV directly on your PC without the need for any of the required UAV hardware. SITL also supports the simulation of other unmanned vehicles such as fixed wing vehicles, ground vehicles, and underwater vehicles. Sensory data for the UAV is calculated and retrieved from a FDM (flight dynamics model) within

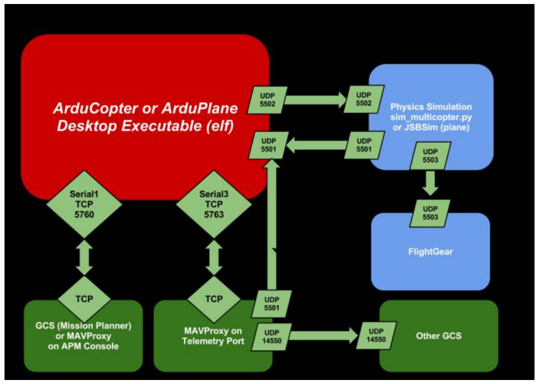

Figure 6: ArduPilot SITL Architecture

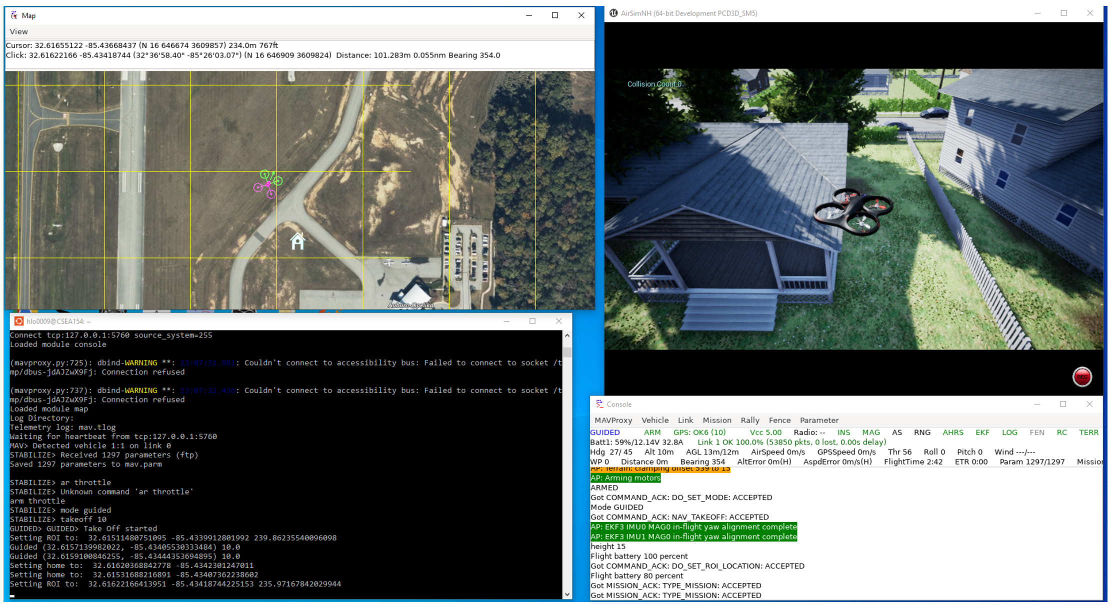

Figure 7: ArduPilot SITL and AirSim

the simulator which is then sent to the autopilot software through either a TCP or UDP port. Information such as the vehicles GPS location, altitude, magnetometer, airspeed, and more are all simulated accurately within SITL. The architecture of software-in-the-loop can be seen in Figure [6]. Microsoft AirSim is an open-source robotics simulation platform developed by Microsoft and is commonly used for data collection which can then be used to train machine learning models for autonomous robotic systems. Using the two pieces of software in combination allows you not only simulate a real world drone inside SITL, but visualize it rather nicely within AirSim as well. However, although SITL can be ran natively on Windows, a WSL (windows subsystem for linux) environment will be needed in order to run ArduPilot SITL and AirSim in Windows together. A representation of running the two pieces of software together can be seen in figure [7]. Using ArduPilot SITL in conjunction with Microsoft AirSim, we were able to simulate our SUAV and train/test a DQN utilized within our path planning effectively.

6 Results

We were able to develop an autonomous SUAV platform equipped with an ArduPilot APM 2.8 flight control unit and thermal imaging capabilities. We were also successful in designing a low-cost 2-axis gimbal stabilizer (Fig. [8]) that can be recreated by anyone with access to 3D modeling software and a hobbyist FDM printer. The SUAV itself hovered steadily at a fixed GPS location as long as there was a solid GPS fix on the vehicle and magnetometer calibration was conducted before each test flight. The aerial video data retrieval system worked as intended and we were able to achieve greater picture quality than as expected when dealing with the 5.8GHz frequency spectrum.

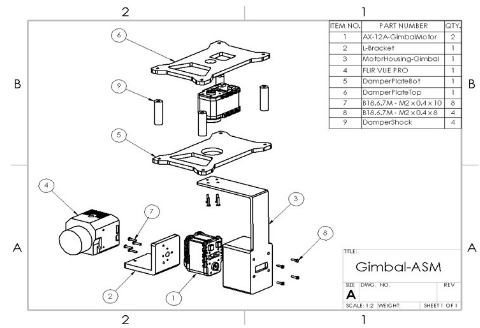

Figure 8: Gimbal Assembly Drawing

Although our path planning model is able to find the target within a relatively short period of time on average, there are still some parameters that could be looked into more in depth within the training and testing in order to add more robustness to the model. Characteristics such as when to explore versus when to exploit is one of these. Another would be to study which action at the beginning of each training epoch would benefit the model the most.

The SSD MobileNet object detection model was tested in cool conditions during the night in order to best simulate the conditions of an SAR rescue during which the thermal imaging would be used. Under such circumstances, the model regularly performed detection with accuracies greater than 95%. The model is equipped to detect multiple people in a frame while maintaining high accuracy and performs comparably well with thermal images taken at altitudes far lower than that of the training data. A visualization of the localization and classification performed with the model can be seen below in Fig. [9]. The images demonstrate real life performance with one or more persons in a SAR environment.

(a) Sample 1 Test

(b) Sample 2 Test

Figure 9: Object Detection Output

7 Conclusion and Future Work

In this research project, we aimed to bolster the effectiveness of rescuer techniques in SAR operations by developing a low-cost UAV-AIS (autonomous intelligent system) or SUAV (smart unmanned aerial vehicle) equipped with stabilized thermal imaging capabilities. Implementing this SUAV system in search and rescue operations can be crucially beneficial to SAR teams who are dealing with short time frames and are searching for missing persons in environments where the use of visible spectrum imaging proves to be a challenge (e.g. smoke, night, light foliage). Our SUAV platform developed for this research can be re-created through relatively simple means so those without the large amount of resources required to attain similar platforms within this field can do so. The designed two-axis gimbal stabilizer was also cost-effective and performed as expected thanks to ArduPilot's native support for gimbal stabilization servo motor control.

Due to the short time frame of the project, we were not able to test the system fully from start to finish in the real world. However, we were able to test each aspect of the system individually and achieved significant results in each. For future work, it is recommended that a three-axis gimbal be used in place of the two-axis gimbal order to accomplish even greater stabilization on the roll axis of the camera. Furthermore, replacing the 5.8GHZ Audio/Video transmitter-receiver pair with something that operates within a lower frequency spectrum such as 2.4GHz or 1.2GHz would extend the range of video data retrieval. Within simulation, it would be possible to attempt the search with a collaborative swarm of UAVs to shorten the duration of the path planning. Collision detection could also be added using the AirSim imaging of the environment. Incorporating infrared imaging from AirSim's computer vision library into the search model would be another possible improvement for future work.

References

[1] J Alanis et al. "Topography and behavior based movement modeling for missing hikers in land-wilderness settings". In: *J. Mathematical Theoretical Biology Institute*. 2019, pp. 1–53.

[2] Marius Beul et al. "Target Chase, Wall Building, and Fire Fighting: Autonomous UAVs of Team NimbRo at MBZIRC 2020". In: *arXiv preprint arXiv:2201.03844* (2022).

[3] Barnabas Gavin Cangan et al. *Anticipatory Human-Robot Path Planning for Search and Rescue*. 2020. DOI: 10.48550/ARXIV.2009.03976. URL: https://arxiv.org/abs/2009.03976.

[4] Jared Doke. "Analysis of search incidents and lost person behavior in Yosemite National Park". PhD thesis. University of Kansas, 2012.

[5] Paul A Dudchenko. *Why people get lost: the psychology and neuroscience of spatial cognition*. Oxford University Press, USA, 2010.

[6] Jianqing Fan et al. "A theoretical analysis of deep Q-learning". In: *Learning for Dynamics and Control*. PMLR. 2020, pp. 486–489.

[7] Amanda Hashimoto et al. "An agent-based model reveals lost person behavior based on data from wilderness search and rescue". In: *Scientific reports* 12.1 (2022), pp. 1–12.

[8] KA Hill. "The psychology of lost". In: *Lost person behavior* 116 (1998).

[9] Robert J Koester. "Lost Person Behavior: A Search and Rescue". In: *dbs Productions LLC* (2008).

[10] Nikite Mesvan. *CNN-based Human Detection for UAVs in Search and Rescue*. 2021. DOI: 10.48550/ARXIV.2110.01930. URL: https://arxiv.org/abs/2110.01930.

[11] Diana Queirós Pokee et al. "Consciousness Detection on Injured Simulated Patients Using Manual and Automatic Classification via Visible and Infrared Imaging". In: *Sensors* 21.24 (2021). ISSN: 1424-8220. DOI: 10.3390/s21248455. URL: https://www.mdpi.com/1424-8220/21/24/8455.

[12] Vidyasagar Sadhu et al. "Aerial-DeepSearch: Distributed Multi-Agent Deep Reinforcement Learning for Search Missions". In: *2020 IEEE 17th International Conference on Mobile Ad Hoc and Sensor Systems (MASS)*. IEEE. 2020, pp. 165–173.

[13] Elena Sava et al. "Evaluating lost person behavior models". In: *Transactions in GIS* 20.1 (2016), pp. 38–53.

[14] Jiashun Suo et al. *HIT-UAV: A High-altitude Infrared Thermal Dataset for Unmanned Aerial Vehicles*. 2022. DOI: 10.48550/ARXIV.2204.03245. URL: https://arxiv.org/abs/2204.03245.

[15] Juan Gonzalo Cárcamo Zuluaga et al. "Deep reinforcement learning for autonomous search and rescue". In: *NAECON 2018-IEEE National Aerospace and Electronics Conference*. IEEE. 2018, pp. 521–524.